Journal of Power Sources 228 (2013) 229–236

Contents lists available at SciVerse ScienceDirect

Journal of Power Sources

journal homepage: www.elsevier.com/locate/jpowsour

Synergy effects of $Pr_{1.91}Ni_{0.71}Cu_{0.24}Ga_{0.05}O_4$ and $Ba_{0.5}La_{0.5}CoO_3$ composite on cathodic activity for intermediate temperature solid oxide fuel cells

Jing Xie [a], Young-Wan Ju [b], Maki Matsuka [c], Shitaro Ida [b,c], Tatsumi Ishihara [c,*]

[a] Department of Automotive Science, Graduate School of Integrated Frontier Science, Kyushu University, 744 Motooka, Nishi-ku, Fukuoka 819-0395, Japan
[b] Department of Applied Chemistry, Faculty of Engineering, Kyushu University, 744 Motooka, Nishi-ku, Fukuoka 819-0395, Japan
[c] International Institute for Carbon Neutral Energy Research (WPI-I2CNER), Kyushu University, 744 Motooka, Nishi-ku, Fukuoka 819-0395, Japan

HIGHLIGHTS

- Synergy effects of mixing Pr_2NiO_4 and $La(Ba)CoO_3$ on cathodic performance were studied.
- Cathodic overpotential could be suppressed by mixing Pr_2NiO_4 with $LaCoO_3$ base oxide.
- The active sites for oxygen dissociation could be extended in three dimensions.
- The maximum power density of 117 mW cm^{-2} was achieved at 673 K with this composite.

ARTICLE INFO

Article history:
Received 1 May 2012
Received in revised form
12 November 2012
Accepted 24 November 2012
Available online 30 November 2012

Keywords:
Cathode
Composite oxide
Pr_2NiO_4
$La(Ba)CoO_3$
Solid oxide fuel cell

ABSTRACT

Synergy effects of mixing Pr_2NiO_4 and $La(Ba)CoO_3$ on cathodic performance were investigated using a $LaGaO_3$-based oxide electrolyte. It was observed that cathodic overpotential could be suppressed significantly by mixing Pr_2NiO_4 with $La(Ba)CoO_3$ base oxide, in spite of a decrease in the electrical conductivity. Because $LaCoO_3$-doped with Ba shows high oxygen dissociation activity and Pr_2NiO_4 shows high oxide ion and hole conductivity, the active sites for oxygen dissociation could be extended in three dimensions. In response to the improved number of active sites, diffusion overpotential was decreased significantly by mixing Pr_2NiO_4-based oxide with $LaCoO_3$-based oxide. The maximum power density of 117 mW cm^{-2} was achieved at temperatures as low as 673 K using a $LaGaO_3$ thin film electrolyte (5-μm thick) and a composite oxide of Pr_2NiO_4–$La(Ba)CoO_3$ cathode.

1. Introduction

Solid oxide fuel cells (SOFCs) are highly efficient and environmentally-friendly power generators with significant advantages. SOFCs are flexible in fuel and also low sensitivity to fuel impurities. SOFCs can be constructed from inexpensive materials and have a long service life [1–5]. However, in terms of cost and durability, SOFCs cannot yet compete with conventional combustion systems. Recently, considerable effort has been expended to improve SOFCs by decreasing the operating temperature. It is expected that a lower operating temperature would suppress the degradation of components, extend the range of acceptable material selection, improve cell durability, and reduce the cost of the system [6]. However, when the operating temperature is decreased, catalytic activity and the kinetics of the electrodes, particularly the oxygen reduction reaction at the cathode, are also decreased [7,8]. Therefore, to improve the catalytic activity of cathode, an active and novel cathode that performs effectively at lower temperatures is highly desirable to improve the catalytic activity of cathode. The main requirements for a cathode are high electronic conductivity, high electrocatalytic activity for the cathode process (oxygen reduction reaction), low vapor pressure during operation, chemical compatibility, an appropriate expansion coefficient, and good adherence to the solid electrolyte [9]. At present, perovskite oxide is widely used as a cathode because of its high surface activity and mixed conductivity. In particular, Co-based perovskite or La(Sr)Fe(Co)O_3 oxide is frequently used [10,11]. Although superior cathodic performance has been achieved by using these oxides, the cathodic overpotential is still large when the cell is operating at temperatures lower than 673 K.

As a potential material, defect perovskite, K_2NiF_4, has been reported to possess a high surface exchange coefficient and a high

* Corresponding author. Fax: +81 92 802 2868.
E-mail address: ishihara@cstf.kyushu-u.ac.jp (T. Ishihara).

0378-7753/$ – see front matter © 2012 Elsevier B.V. All rights reserved.
http://dx.doi.org/10.1016/j.jpowsour.2012.11.089

oxygen diffusion coefficient because of its unique structure [12–14], i.e., series connection of perovskite and rock salt block. Therefore, this oxide group is attracting strong interest as a new class of cathode [15–17]. In our previous study, the mixed conductivity and oxygen permeation properties of Pr-deficient $Pr_{1.9}Ni_{0.71}Cu_{0.24}M_{0.05}O_{4+\delta}$ (M = In, Ga, Al, and Ni) were investigated [18–21]. Among the dopants studied, Ga-doped material showed superior mixed conductivity and exhibited a higher oxygen permeation rate compared with that of the other materials. $Pr_{1.9}Ni_{0.71}Cu_{0.24}Ga_{0.05}O_{4+\delta}$ (PNCG) had the highest oxygen permeation rate of 286 μmol min^{-1} cm^{-2} (ca. 7 cm^3 min^{-1} cm^{-2}) from air to He at 1273 K in a 0.5 mm thick membrane [21]. However, the surface activity for oxygen dissociation of PNCG is not large. Thus, in order to achieve a high oxygen permeation rate, a more effective surface catalyst is essential and in our previous study, $La_{0.9}Sr_{0.1}Co_{0.8}Fe_{0.2}O_3$ (LSCF) was used for surface catalyst for achieving high oxygen permeation rate. Because of high oxide ion conductivity, the combination of PNCG with an active catalyst enhances the process of oxygen dissociation, which offers a new and very interesting active cathode material. In this study, the cathodic activity of composite oxides containing PNCG was investigated. These composite oxides possess high oxide ion conductivity. The reactivity and electrical conductivity properties of the mixed oxides containing PNCG were also studied.

2. Experiments

The electrolyte used in this study was $La_{0.9}Sr_{0.1}Ga_{0.8}Ma_{0.2}O_3$ (denoted as LSGM), which was prepared by a conventional solid state reaction technique using La_2O_3, $SrCO_3$, Ga_2O_3, and MgO as starting reagents. Details of the preparation method can be found elsewhere [22]. The final sintering temperature was 1773 K for 6 h in air. The obtained disks were ground to 0.3 mm in thickness using a diamond grinding machine. $Pr_{1.9}Ni_{0.71}Cu_{0.24}Ga_{0.05}O_{4+\delta}$ (PNCG) was also prepared by the solid state reaction method. Appropriate amounts of nitrates were first dissolved in distilled water followed by stirring, heating, and drying. The dry powder obtained was calcined at 673 K for 2 h to decompose nitrate acid. Next, the obtained powder was ground in an alumina mortar. After grinding, the resultant product was calcined at 1473 K for 6 h. In this study, different oxides were mixed with PNCG as a composite candidate cathode for intermediate temperature SOFC. The prepared PNCG was mixed with 8 mol% yttrium stabilized ZrO_2 (YSZ), $Sm_{0.2}Ce_{0.8}O_2$ (SDC), $Ba_{0.5}La_{0.5}CoO_3$ (BLC), $Sm_{0.5}Sr_{0.5}CoO_3$ (SSC), or $La_{0.9}Sr_{0.1}Co_{0.8}Fe_{0.2}O_3$ (LSCF) at weight ratio 1:1 using a planetary ball mill mixer at 300 rpm for 1 h in air. In this study, the composite cathodes of PNCG and BLC composites were further studied at the weight ratio 1:1, 1:2, 1:3, 1:5, or 1:9.

A single planar-type SOFC with an effective electrode area of 0.12 cm^2 was prepared. A composite oxide cathode and Ni–Fe oxide, as an anode precursor, were painted on each face of the LSGM electrolyte disk. Cathode and anode powder were mixed with *n*-butyl acetate in order to prepare the electrode ink. Next, the electrode ink was painted on the electrolyte surface by hand. A platinum mesh (80 mesh) was then pushed into the electrode with a mullite tube for the current corrector. A platinum wire was attached close to the cathode using a platinum paste (Tanaka TR7902) and was used as the reference electrode. After painting the electrodes, the cell was fired at 1273 K for 40 min to remove the organic solvent and improve the interface contact between electrodes and electrolyte. Before the cell performance measurement, the Ni–Fe anode was reduced to a metallic state at 1073 K for 1 h under H_2 flow (100 ml min^{-1}). Pure O_2 and hydrogen humidified with 3 vol% H_2O were fed to the cathode and the anode, respectively. The power generation characteristics were measured by the four-probe method. A galvanostat (Hokuto, HA–301) was used to provide the electrical load. Internal resistance was measured by a current interruption method and AC impedance. A current pulse was generated using a current pulse generator (Hokuto, HC–111) and the corresponding potential response was measured with a Memory HiCORDER (Hioki, 8835). The electrochemical impedance spectra were also measured with an impedance analyzer (Solatron 1260) with a controllable galvanostat/potentiostat, model 1287. The thin film electrolyte cell was also tested to estimate the cathodic property at lower temperatures. The thin film was prepared on a Ni–Fe porous metal substrate using PLD method. Details of the preparation method have been described elsewhere [23].

Table 1
Maximum power density and cathodic potential drop by IR loss and overpotential on the cell using composite cathode.

Cathodes	M.P.D. (mW cm^{-2})	IR loss (mV)	η_c (mV)	M.P.D (mW cm^{-2})	IR loss (mV)	η_c (mV)
	1073 K			973 K		
PNCG	543.8	43.20	48.30	266.7	61.58	75.70
BLC	975.0	16.22	13.76	366.7	14.89	23.44
SSC	1106.0	6.70	13.40	416.7	17.70	24.20
YSZ–PNCG (1:1)	2.10	–	–	–	–	–
SDC–PNCG (1:1)	39.60	129.93[a]	41.74[a]	15.00	78.56[b]	63.02[b]
LSGM–PNCG (1:1)	114.60	196.20	73.63	29.50	97.15[a]	98.90[a]
LSCF–PNCG (1:1)	616.70	18.29	32.61	279.20	37.50	55.70
SSC–PNCG (1:1)	712.50	6.73	24.85	308.30	12.11	44.66
BLC–PNCG (1:1)	631.30	14.12	8.56	355.00	21.92	31.53
Cathodes	873 K			773 K		
PNCG	60.4	143.50	130.90	8.3	–	–
BLC	102.1	26.38	25.01	18.3	–	–
SSC	90.0	46.40	39.80	19.3	63.30	19.16
YSZ–PNCG (1:1)	–	–	–	–	–	–
SDC–PNCG (1:1)	5.40	90.85[c]	91.66[c]	1.20	–	–
LSGM–PNCG (1:1)	7.30	75.90[b]	92.10[b]	1.50	–	–
LSCF–PNCG (1:1)	85.40	–	–	–	–	–
SSC–PNCG (1:1)	103.30	–	–	–	–	–
BLC–PNCG (1:1)	125.00	47.07	32.08	23.50	39.07	85.07

The values at 1073, 973, and 873 K were recorded at 0.1 A cm^{-2}, and the values at 500 °C was recorded at 30 mA cm^{-2}, [a] 30 mA cm^{-2}, [b] 10 mA cm^{-2}, [c] 5 mA cm^{-2}, respectively.
YSZ: 8 mol% yttrium stabilized ZrO_2; SDC: $Sm_{0.2}Ce_{0.8}O_2$, LSCF: $La_{0.1}Sr_{0.9}Co_{0.2}Fe_{0.8}O_3$; SSC: $Sm_{0.5}Sr_{0.5}CoO_3$; BLC: $Ba_{0.5}La_{0.5}CoO_3$; PNCG: $Pr_{1.91}Ni_{0.71}Cu_{0.24}Ga_{0.05}O_4$.

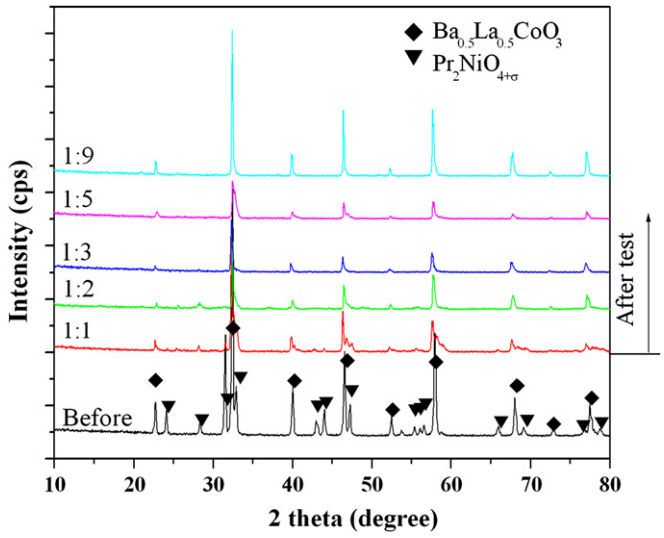

Fig. 1. XRD pattern of composite oxides of PNCG and BLC before and after the cell test.

The conductivity was measured using a DC 4-probe method with Pt electrodes. The thermal expansion coefficient (TEC) of the dense samples was also measured with commercial thermal mechanical analysis system (Thermal plus TMA 8310) with Al_2O_3 as a reference. Each sample was heated from room temperature to 1273 K at a rate of 10 K min^{-1} in air.

3. Results and discussion

3.1. Cathodic property of PNCG-based composite oxide on LSGM electrolyte

Table 1 is a summary of power density of the cell examined with various cathodes. In addition, it comprises the details of the internal resistance of cells using various composite oxide cathodes containing PNCG. In first step study, all composite oxides were mixed with 50 wt% PNCG; Ni–Fe (9:1) powder was always used as the anode. Maximum power density (M.P.D.) was noted as the maximum power density. IR loss and η_c were cathodic IR loss and cathodic overpotential, respectively. As shown in Table 1, the power densities of the cathode materials varied drastically. First, PNCG shows reasonably cathodic performance at high temperature, but not good as compared to the conventional active perovskite oxides, SSC, or BLC. This reasonable cathodic performance could be assigned to the high oxide ion conductivity of PNCG. However, cathodic overpotential increased significantly with decreasing operating temperature, and a negligibly small power density is exhibited at 773 K by the cell with the PNCG cathode.

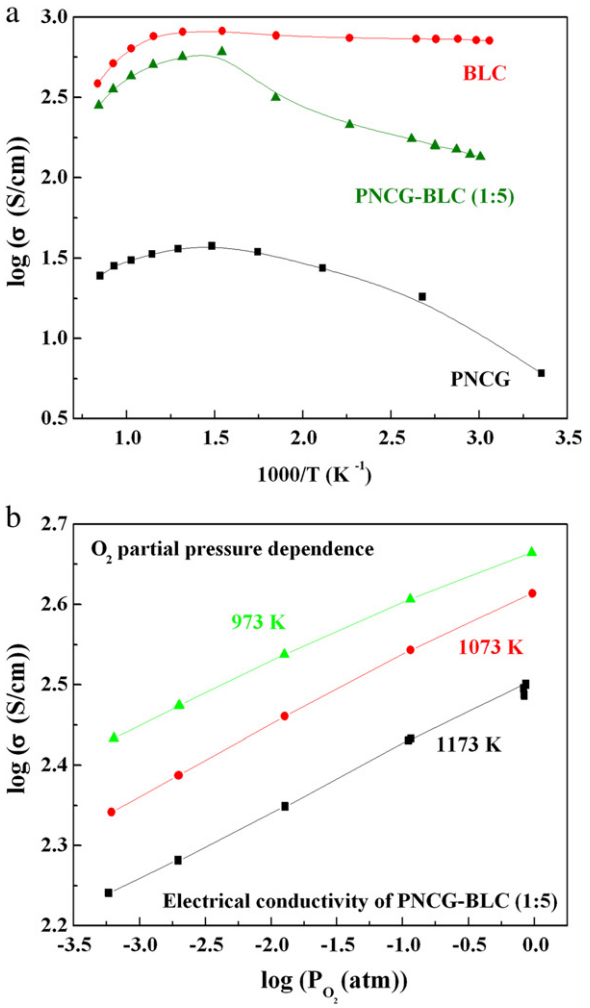

Fig. 2. Electrical conductivity as a function of temperature (a) and electrical conductivity as a function of oxygen partial pressure (b).

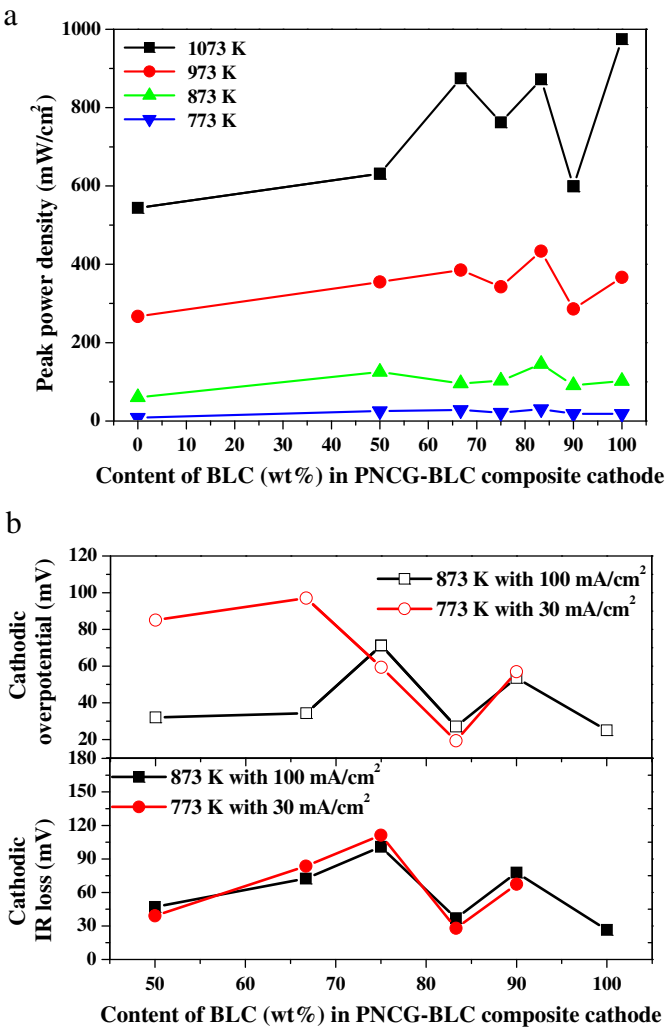

Fig. 3. Maximum power density (a) cathodic IR loss and overpotential (b) as a function of BLC content (wt%) in PNCG–BLC composite cathode.

This suggests that the surface activity of PNCG for oxygen dissociation is not high compared with that of BLC or SSC perovskite oxide, particularly at lower temperatures. In contrast, reasonably high power density and small overpotential were observed on the cell using the BLC or SSC cathode. Table 1 shows the power density as well as the cathode performance of the composite oxide containing PNCG. Evidently, mixing PNCG with an oxide ion conductor results in a much smaller power density, which is reasonable because PNCG originally shows high oxide ion conductivity. On the other hand, as expected, the power density at lower temperature range was improved by mixing PNCG with a typical perovskite cathode oxide. At 1073 K, the cell with PNCG–SSC showed higher power density than that of the cell with the PNCG–LSCF or PNCG–BLC cathode. However, when the cell operating temperature decreased to 973 and 873 K, the cell with the PNCG–BLC cathode showed higher power density and smaller cathodic overpotential among the examined mixed oxide cathodes. It is notable that at 773 K, the power density of the cell with the PNCG–BLC cathode reached 23.5 mW cm^{-2} in spite of using a thick electrolyte (0.3 mm). The IR loss of PNCG–BLC was lower than that of PNCG–LSCF and a little higher than that of the PNCG–SSC cathode. However, compared to the cells with PNCG–LSCF or PNCG–SSC, the cathodic overpotential of PNCG–BLC was obviously lower at all temperature ranges. This indicates that a combination of PNCG and BLC is highly effective for increasing the cathodic performance and cell performance. Therefore, the cathodic performance of the composite oxide of PNCG–BLC was studied in more detail. It is also noted that comparing with BLC, IR loss of BLC–PNCG composite is little larger at low current density, but became smaller at high current density.

Fig. 1 shows XRD patterns of the composite oxide of PNCG–BLC before and after cell performance measurement. As shown in Fig. 1, no change was observed in the diffraction patterns before the cell test, which suggests that no reaction between BLC and PNCG oxide was recognized. Although small diffraction peaks were observed after the cell test, large diffraction peaks could be assigned to BLC and PNCG. At present, details analysis for small diffractions peaks were not performed because of weak intensity.

Electrical conductivity of PNCG, BLC, and their composite were measured as a function of temperature and oxygen partial pressure. Fig. 2(a) shows the temperature dependence of the electrical conductivity of PNCG, BLC, and PNCG–BLC (1:5) composite. The conductivities of both PNCG and BLC increased in the low temperature region as the temperature increased and then decreased as the temperature increased further. Therefore, for both BLC and PNCG, semiconductor-like performance dominates at low temperatures and metallic-like performance dominates at high temperatures. On the other hand, the PNCG–BLC composite has an intermediate conductivity between parent oxides. At low temperatures, electrical conductivity of the PNCG–BLC composite is much higher than that of PNCG but is still lower than that of BLC. Considering the simple mixture of BLC and PNCG, the intermediate conductivity between BLC and PNCG is quite reasonable. However, the observed conductivity is higher than that of the simple averaged values of PNCG and BLC at high temperatures and is much lower at low temperatures. Therefore, the main hole conduction path could be assigned to the BLC powder, which has higher conductivity than that of PNCG at high temperature. In contrast, in low temperature regions, conductivity increases with increasing temperature, which is similar to the performance of PNCG. Therefore, electrical conductivity in the PNCG–BLC composite is more strongly affected by PNCG because of the resistive component in the composite oxide at low temperatures. Fig. 2(b) shows the O_2 partial pressure dependence of the PNCG–BLC composite. The conductivity decreased with decreasing O_2 partial pressure. The O_2 partial pressure dependence is around 1/10, which is close to that of PNCG. Therefore, the hole conductivity is dominant in this oxide and the hole conductivity is strongly affected by the PNCG phase. Because the conductivity, log σ (S cm^{-1}), is always greater than 2, it is evident that the composite oxide of BLC and PNCG shows reasonably high value as an electrode material.

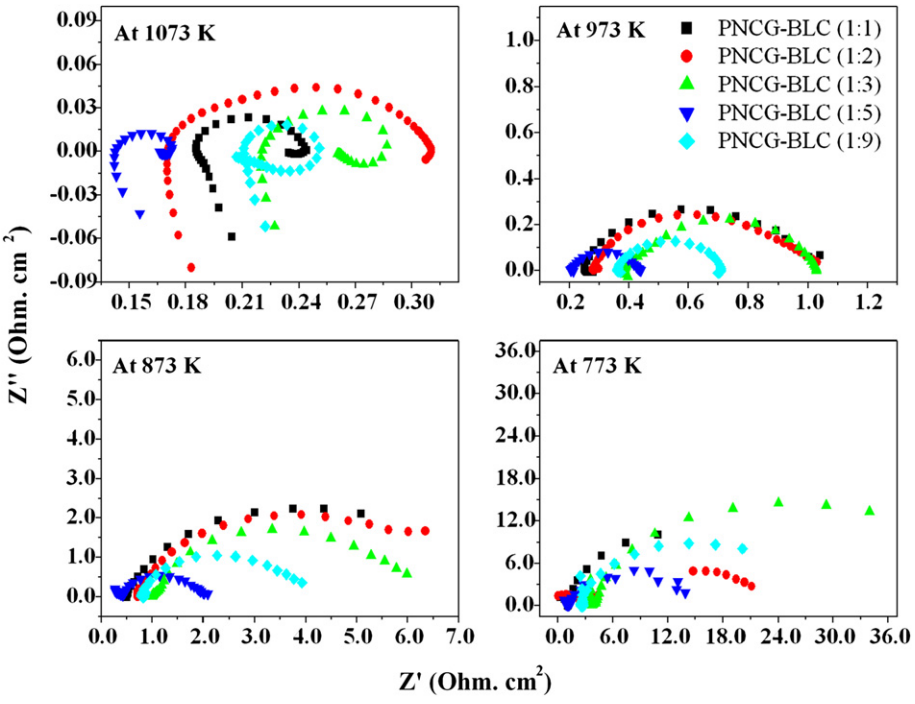

Fig. 4. Complex impedance plots for cells with different composite cathodes.

The effects of the composition of the PNCG–BLC composite oxide on power generating properties were studied. Fig. 3(a) shows the maximum power density of the cell as a function of the BLC content. The highest power density for PNCG–BLC (1:2) was obtained at 1073 K. The power densities obtained at 973 K and 873 K were almost independent of the composition. However, at temperatures lower than 773 K, the power density became slightly higher for PNCG–BLC (1:5). In this study, our objective was to develop active cathode material for low temperature operations. The optimized composition ratio for a PNCG–BLC cathode seems to exist at PNCG–BLC (1:5).

Fig. 3(b) shows the cathodic IR loss and overpotential of cells at 873 and 773 K, as a function of BLC content in PNCG–BLC composite oxide. Evidently the values obtained for IR loss and overpotential became smallest when the composition ratio of PNCG–BLC was 1:5, which shows the largest power density at low temperatures. Therefore, higher power density could be assigned to the small IR loss and overpotential. Although the electrical conductivity of PNCG–BLC is lower than that of BLC, as shown in Fig. 3(a), smaller IR loss on the composite oxide is highly interesting because it exhibits lower electrical conductivity than that of BLC. The composition ratio of PNCG–BLC is 1:5, which is considered to be the optimized composition ratio for cathode and is studied in further detail. It is also noted that we measured for several times of cathodic performance of BLC–PNCG composite cathode and the results were agreed in the experimental error.

Table 2
Area specific resistance estimated from impedance spectra.

Temp. (K)	PNCG–BLC (1:5)			BLC		
	ASR (Ω cm^2)	ASR_H (Ω cm^2)	ASR_L (Ω cm^2)	ASR (Ω cm^2)	ASR_H (Ω cm^2)	ASR_L (Ω cm^2)
1073 K	0.03	–	0.03	0.33	0.1	0.23
973 K	0.23	–	0.23	1.57	0.14	1.43
873 K	3.48	1.38	2.1	21.6	7.03	14.57

BLC: $Ba_{0.5}La_{0.5}CoO_3$; PNCG: $Pr_{1.91}Ni_{0.71}Cu_{0.24}Ga_{0.05}O_4$.
PNCG–BLC (1:5) means the mixed ratio of PNCG to BLC is 1:5.
Note: $ASR = ASR_H + ASR_L$.

AC impedance is an effective technique for analyzing the reaction step in an electrode reaction. Applying AC impedance in electrochemical systems can also provide detailed information about the electrochemical reactions on the electrode. Fig. 4 shows the complex impedance plots for cathodes with different compositions. A depressed semicircle was observed for cathodic impedance, suggesting that at least two reaction steps exist on cathode. Resistance corresponding to the *x* axis intercept of the semicircle in the high frequency region, which was primarily assigned to the contact and material electrode resistance, was strongly dependent on the composition of the composite oxide. Because the electrical conductivity of the materials is not simply related to that of the observed electrode resistance, interface resistance could be the main component of electrode resistance. Evidently, at 1073 K, electrode resistance is much larger than that of electrode overpotential, which is estimated from the diameter of the semicircle. Therefore, at 1073 K, overpotential of the electrode is negligibly small. On the other hand, with decreasing operating temperatures, resistance corresponding to the diameter of the semicircle became larger, suggesting insufficient cathodic activity. At all temperatures, PNCG–BLC composite with a composition ratio of 1:5 showed the smallest semicircle (Fig. 5).

For the impedance spectra, the low frequency arc is generally corresponding to a diffusion overpotential. It can be seen that, the arcs at the low frequency part are much larger than that at high frequency region for BLC. This means that oxygen diffusion and dissociation process are the dominating step of the oxygen reduction reaction rate on BLC. The area specific resistance calculated from the impedance spectra was summarized in Table 2 for both oxides. As shown in Table 2, compared with BLC, the resistance of BLC–PNCG composite cathode shows the smaller charge transfer

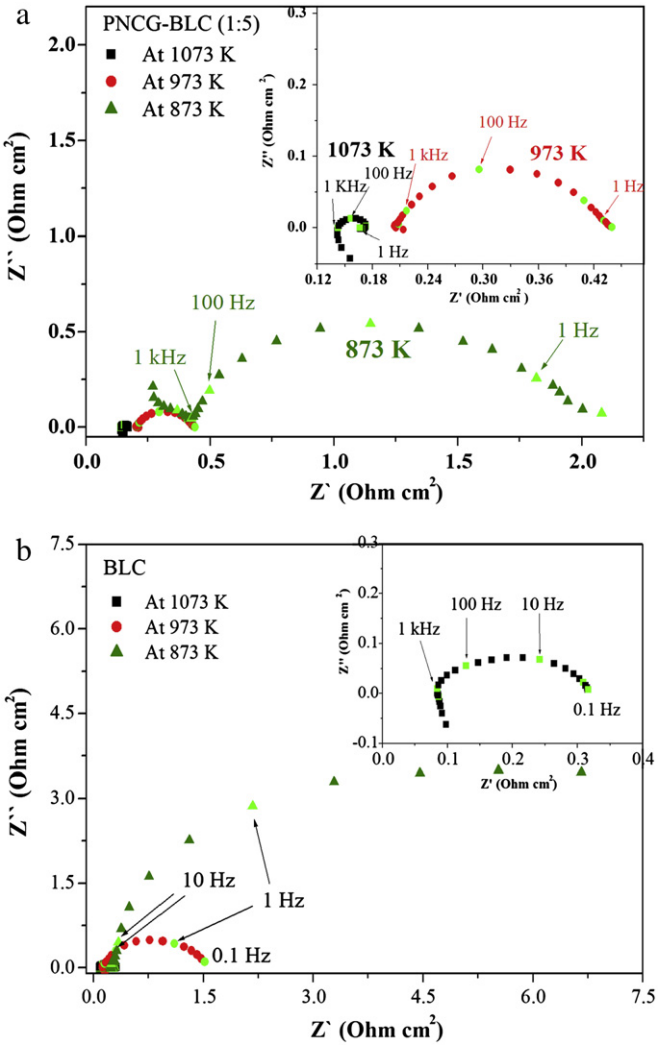

Fig. 5. Complex impedance plots of cathodic impedance spectra of the cell using (a) PNCG–BLC (1:5), and (b) BLC.

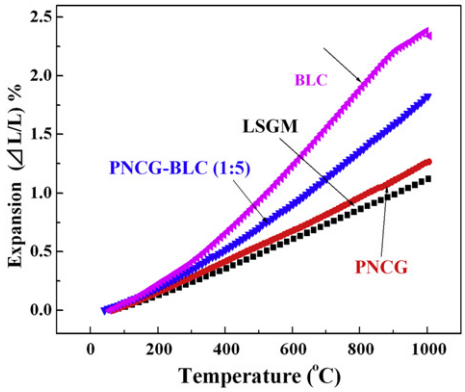

Fig. 6. Thermal expansion coefficient of BLC, PNCG–BLC (1:5), PNCG, and LSGM as a function of temperature.

resistance, however, that assigned to diffusion overpotential became much smaller suggesting that decrease in diffusion resistance mainly assigned to the improved cathodic performance of BLC–PNCG.

The compatibility of the PNCG–BLC composite oxide was further studied. Fig. 6 shows the thermal expansion property of the PNCG–BLC composite oxide. It is well known that the TEC of Co-based perovskite oxide is much larger than that of an LSGM electrolyte [11]. In particular, the TEC of BLC is much larger than that of LSGM. Therefore, one reason why BLC possesses a large contact resistance might be assigned to the partial delamination of the cathode. It is highly interesting that the TEC of PNCG–BLC (1:5) is much closer to that of LSGM because PNCG and LSGM have similar TECs. Therefore, in relation to TEC, the compatibility of the PNCG–BLC composite with the LSGM electrolyte is reasonably high. Therefore, one reason for decreased IR loss might be assigned to the improved thermal expansion property.

3.2. Cathodic performance of PNCG–BLC at decreased temperature

It is suggested that the composite oxide of PNCG–BLC is useful as a cathode material at intermediate temperatures. Thus, the performance of the composite oxide of PNCG–BLC at lower temperatures was studied. Because of the large IR loss from the electrolyte, the cell using the 5-μm-thick LSGM electrolyte, which was prepared with PLD method, was used. Preparation of the LSGM thin film was performed using the PLD method. Details of the method have been reported previously [23]. Fig. 7 shows a SEM image of the film prepared on a porous Ni–Fe porous metal substrate. Evidently, thin but dense LSGM electrolyte film was prepared successfully using the PLD method. In the previous study, we used an SSC cathode to measure power generating performance, and it was found that the reasonably high power density was achieved by this cell [23].

Fig. 8 shows *I–V* and *I–P* curves of the cell using BLC, SSC, and PNCG–BLC (1:5) composite oxide at 773 and 673 K. At both temperatures, the cell using the PNCG–BLC cathode shows the highest power density. Differences in power density became larger with decreasing operating temperatures. In particular, at 673 K, the maximum power density of the cell using the PNCG–BLC composite was almost double of that of the SSC cathode. Therefore, evidently, PNCG–BLC composite oxide is highly promising as an active cathode for intermediate temperature SOFCs. Considering the maximum power density of 0.25 W cm^{-2} for a commercial SOFC (Westinghouse) at 1273 K [2], the maximum power density of 0.12 W cm^{-2} suggests that an SOFC can be operated at 673 K by using an LSGM thin film and a PNCG–BLC composite oxide cathode.

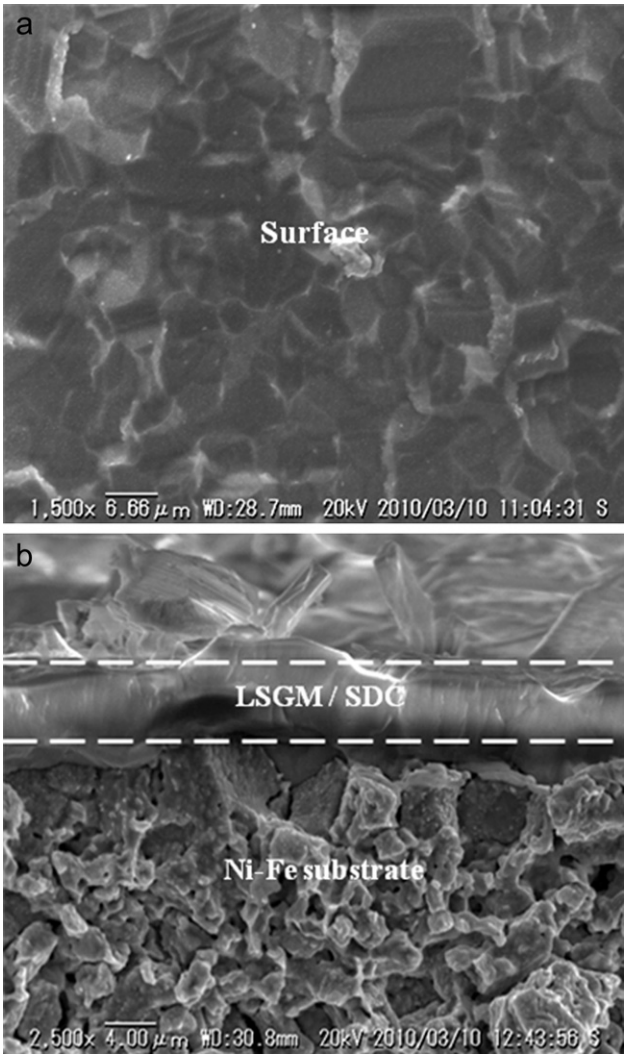

Fig. 7. SEM image of a metal supported cell; (a) surface morphology of electrolyte and (b) cross-section image.

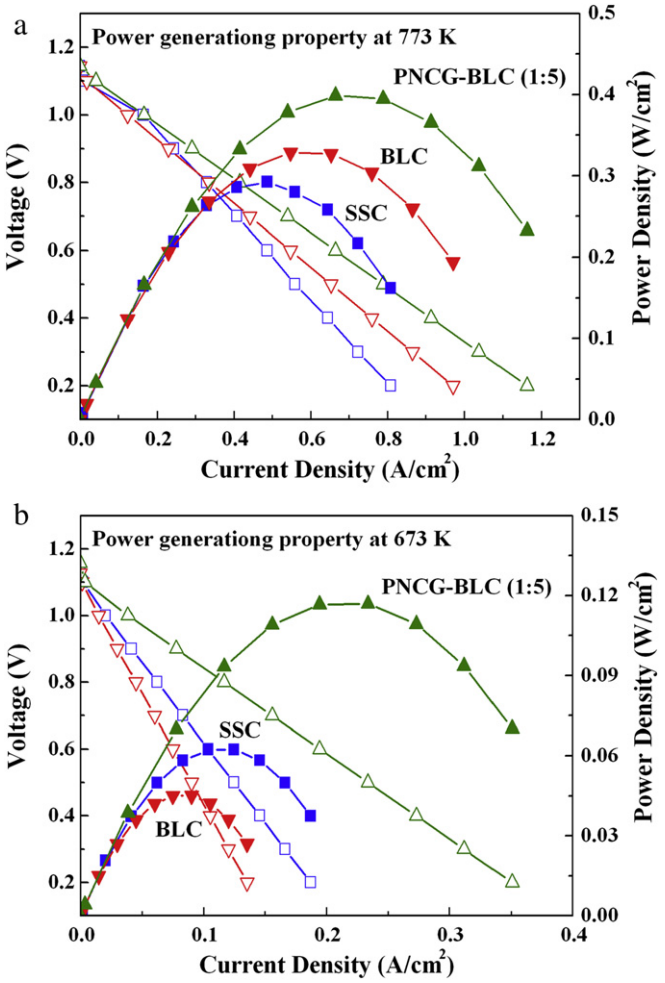

Fig. 8. *I–V* and *I–P* curves of cell with SSC, BLC, PNCG–BLC at 500 °C (a) and 400 °C (b).

The internal resistance of the cell at 673 K was also studied using the current interruption method. Fig. 9(a) shows cathodic and anodic overpotential and IR loss of BLC and PNCG–BLC as a function of current density at 673 K. Because 5-μm-thick LSGM film was used for the cell, the process of separating cathode and anode overpotential with the reference electrode might not have been perfect. However, considering the observed overpotential, the cathodic overpotential is larger than that of the anodic overpotential. Therefore, it makes one thing clear that at 673 K, the primary factor for cell performance in our experiments was the cathodic polarization. With the current interruption method, the polarization of cathode was separated to IR loss and overpotential, Although IR loss is the predominant internal resistance at high temperature, we observed that electrode overpotential becomes dominant and larger at 673 K, and consequently electrode reaction becomes slower with decreasing operating temperature. Therefore, the PNCG–BLC composite oxide showed smaller cathodic overpotential at 673 K. For comparison, details of cathodic overpotential of the cell using a single BLC oxide for cathode are shown in Fig. 9(b). Evidently, the potential drop of cathodic overpotential is almost half of that of BLC. The high power density of the cell using the PNCG–BLC composite cathode could be assigned to the small cathodic overpotential.

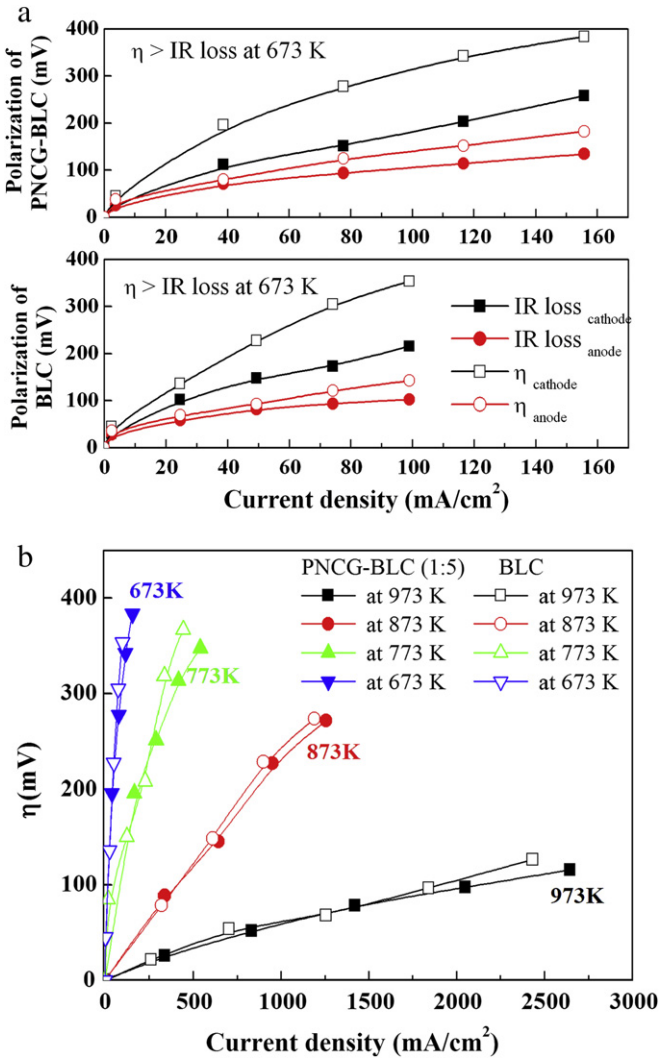

Fig. 9. Polarization of BLC and PNCG–BLC (1:5) as a function of current density, a) anodic and cathodic polarization of BLC and PNCG–BLC (1:5) at 673 K, b) cathodic overpotential of BLC and PNCG–BLC (1:5) at all temperatures.

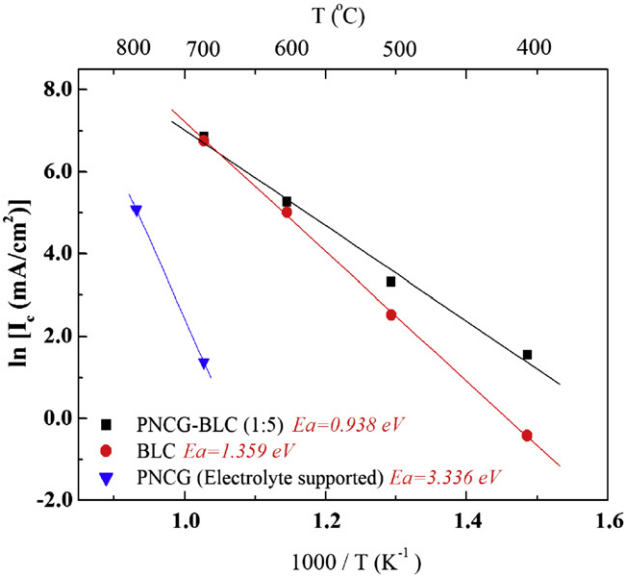

Fig. 10. Arrhenius plots of cathode current density at an overpotential (η_c) of 0.05 V for PNCG–BLC (1:5), BLC, and PNCG (electrolyte supported).

To identify the reason for decreased cathodic overpotential, which is obtained by combining BLC and PNCG, apparent activation energy for the cathodic reaction was estimated. Fig. 10 shows the Arrhenius plots of the current density at an overpotential of 50 mV. Since surface activity of PNCG is not high, Arrhenius plots for PNCG is limited at temperature higher than 973 K. The activation energy for the apparent electrode reaction could be estimated from the slope of the plots in Fig. 10. For BLC, the estimated activation energy, Ea_{BLC}, is 1.359 eV. On the other hand, the estimated activation energy, $Ea_{PNCG-BLC}$, for the PNCG–BLC composite oxide is 0.938 eV. Evidently, by mixing PNCG with BLC, the apparent activation energy for cathodic reaction decreased by almost 2/3 for BLC and 1/3 for PNCG. This suggests that the activity for oxygen molecule dissociation into the oxide ion, i.e., surface activity of the cathode catalyst, per unit site is much improved. Although the PNCG–BLC composite oxide is simply a mixture, large synergy effects were observed for surface activity and this could be related to high oxide ion conductivity in PNCG. Compared to BLC, PNCG shows much higher oxide ion conductivity. Therefore, the number of reaction sites could be improved in three dimensions by mixing active BLC with PNCG. As a consequence, the concentration of current density at the narrow three phase boundary could decrease, which resulted in improved activity for the cathodic reaction. It is reasonable to conclude that the PNCG–BLC composite is highly active for the cathode reaction at low temperatures because of the improved number of reaction sites.

4. Conclusions

In this study, the synergy effects of a mixed conductor of $Pr_2Ni(Cu, Ga)O_4$ and $La(Ba)CoO_3$ were investigated for cathode activity at low temperature operation of SOFCs. It was found that cathodic overpotential became much smaller by mixing PNCG and BLC, which resulted in a much higher power density at 673 K. Because PNCG shows high oxide ion conductivity and BLC shows high activity for oxygen dissociation, mixing a PNCG oxide with BLC is effective for extending the reaction site in three dimensions. Positive effects of combination is not a simply sum of both materials

but much improved cathodic performance was observed. Therefore, synergy effects were observed for BLC–PNCG composite oxide. In response to the increased number of reaction sites, an impedance semicircle in the low frequency region, which is assigned to diffusion resistance, decreased significantly for the composite oxide. In addition, compatibility in thermal expansion property is also improved by mixing PNCG with BLC. Consequently, this study reveals that a composite oxide, PNCG–BLC (1:5), is promising as an active cathode for SOFCs, which uses a $LaGaO_3$ base electrolyte. The maximum power density of 117 mW cm^{-2} was exhibited at temperatures as low as 673 K using PNCG–BLC (1:5) and a 5-μm-thick $LaGaO_3$ film for the cathode and electrolyte, respectively.

References

[1] B.C.H. Steele, K.M. Hori, S. Uchino, Solid State Ionics 135 (2000) 445.
[2] N.Q. Minh, J. Am. Ceram Soc. 76 (1993) 563.
[3] R.A. DeSouza, J.A. Kilner, Solid State Ionics 106 (1998) 175.
[4] S.C. Singhal, Solid State Ionics 152–153 (2002) 405.
[5] Y. Mizutani, K. Hisada, K. Ukai, H. Sumi, M. Yokoyama, Y. Nakamura, et al., J. Alloys Compd 408–412 (2006) 518.
[6] C.W. Sun, R. Hui, J. Roller, J. Solid State Electrochem. 14 (2010) 1125.
[7] J. Fleig, Annu. Rev. Mater. Res. 33 (2003) 361.
[8] M. Kubicek, A. Limbeck, T. Fromling, H. Hutter, J. Fleig, J. Electrochem. Soc. 158 (6) (2011) B727.
[9] A. Rolle, S. Boulfrad, K. Nagasawa, H. Nakatsugawa, O. Mentre, J. Irvine, D.-M. Sylvie, J. Power Sources 196 (2011) 7328.
[10] H. Arai, T. Yamada, K. Eguchi, T. Seiyama, Appl. Catal. 26 (1986) 265.
[11] T. Ishihara, Perovskite Oxide for Solid Oxide Fuel Cells (2009), ISBN 978-0-387-77707-8.
[12] S.J. Skinner, J.A. Kilner, Solid State Ionics 135 (2000) 709.
[13] E. Boehm, J.-M. Bassat, P. Dordor, F. Mauvy, J.-C. Grenier, P. Stevens, Solid State Ionics 176 (2005) 2717.
[14] J.A. Kilner, C.K.M. Shaw, Solid State Ionics 154–155 (2005) 523.
[15] C. Ferchaud, J.C. Grenier, Z.-S. Ye, Marc M.A. van Tuel, Frans PF. van Berkel, J.-M. Bassat, J. Power Sources 196 (2011) 1872.
[16] V.V. Kharton, A.P. Viskup, A.V. Kovalevsky, E.N. Naumovich, F.M.B. Marques, Solid State Ionics 143 (2001) 337.
[17] D. Pérez-Coll, A. Aguadero, M.J. Escudero, P. Núñez, L. Daza, J. Power Sources 178 (2008) 151.
[18] T. Ishihara, S. Miyoshi, T. Furuno, O. Sanguanruang, H. Matsumoto, Solid State Ionics 177 (2006) 3087.
[19] T. Ishihara, K. Nakashima, S. Okada, M. Enoki, H. Matsumoto, Solid State Ionics 179 (2008) 1367.
[20] M. Yashima, M. Enoki, T. Wakita, R. Ali, Y. Matsushita, F. Izumi, T. Ishihara, J. Am. Chem. Soc. 130 (2008) 2762.
[21] M. Yashima, N. Sirikanda, T. Ishihara, J. Am. Chem. Soc. 132 (2010) 2385.
[22] T. Ishihara, H. Matsuda, Y. Takita, J. Am. Chem. Soc. 116 (1994) 3801.
[23] Y.-W. Ju, H. Eto, T. Inagaki, I. Shitaro, T. Ishihara, J. Power Sources 195 (2010) 6294.